

Investigation of drift effect on silicon nanowire field effect transistor based pH sensor

This content has been downloaded from IOPscience. Please scroll down to see the full text.

2016 Jpn. J. Appl. Phys. 55 06GG01

(<http://iopscience.iop.org/1347-4065/55/6S1/06GG01>)

View [the table of contents for this issue](#), or go to the [journal homepage](#) for more

Download details:

IP Address: 147.46.117.86

This content was downloaded on 29/07/2016 at 07:02

Please note that [terms and conditions apply](#).



Investigation of drift effect on silicon nanowire field effect transistor based pH sensor

Sihyun Kim¹, Dae Woong Kwon¹, Ryoongbin Lee¹, Dae Hwan Kim², and Byung-Gook Park^{1*}

¹Inter-University Semiconductor Research Center (ISRC) and Department of Electrical Engineering and Computer Science (EECS), Seoul National University, Seoul 151-742, Korea

²School of Electrical Engineering, Kookmin University, Seoul 136-702, Republic of Korea

*E-mail: bgpark@snu.ac.kr

Received November 30, 2015; revised January 11, 2016; accepted January 13, 2016; published online April 8, 2016

It is widely accepted that the operation mechanism of pH-sensitive ion sensitive field effect transistor (ISFET) can be divided into three categories; reaction of surface sites, chemical modification of insulator surface, and ionic diffusion into the bulk of insulator. The first mechanism is considered as the main operation mechanism of pH sensors due to fast response, while the others with relatively slow responses disturb accurate pH detection. In this study, the slow responses (often called drift effects) are investigated in silicon nanowire (SiNW) pH-sensitive ISFETs. Based on the dependence on the channel type of SiNW, liquid gate bias, and pH, it is clearly revealed that the drift of n-type SiNW results from H⁺ diffusion into the insulator whereas that of p-type SiNW is caused by chemical modification (hydration) of the insulator.

© 2016 The Japan Society of Applied Physics

1. Introduction

Since the development of nano-fabrication technology, biomedical detection devices which can detect small biological entities such as DNA, proteins and virus have been widely researched.¹⁻⁴⁾ Among the biomedical detection devices, silicon nanowire (SiNW) FET based biosensor has been considered as a promising device due to its merits of high sensitivity, low-cost, mass producibility, and real-time detection which originate from its high surface-to-volume ratio and rapid depletion/accumulation of charges.⁵⁻²⁰⁾ In addition, SiNW biosensors can be co-integrated with CMOS (for read-out circuit) by top-down fabrication process.²¹⁾

Despite these advantages, challenges still remain for commercialization as chemical/biomedical sensors. Particularly, unstable operation by current drift (change of drain current with measurement time under a fixed bias) has been one of the main obstacles. As a matter of fact, in repeated detections of pH, the measured drain current (I_D) increases or decreases, which prevents accurate pH detection.^{20,22)} Drift effect may be generally due to one or more of following causes: field enhanced ion migration within the insulator, injection of electrons from the electrolyte, slow surface effects, and bulk ionic diffusion.²³⁻²⁶⁾ However, these explanations have limited measurement data in terms of channel type. In this study, the underlying physical causes of the drift effect are thoroughly analyzed with fabricated (both n- and p-types) SiNW biosensors by measuring time-dependent I_D under various pH and liquid gate biases.

2. Experimental methods

Top-down fabrication was used for SiNW ISFETs, which enables CMOS-compatible fabrication and accurate nanowire alignment.²⁷⁾ The schematic diagram of the fabricated SiNW ISFET with co-integrated CMOS is shown in Fig. 1(a). With an exception of the sensing area opening, all the process steps were conducted simultaneously.

The process flow is illustrated in Fig. 1(b). Devices were fabricated on $1 \times 10^{15} \text{ cm}^{-3}$ boron doped (100) silicon-on-insulator (SOI) wafers to efficiently define silicon nano-wire channels. After a buffer oxidation, channel was implanted with boron and phosphorus on each region of the SOI wafers to adjust threshold voltages (V_{th}) of n-type/p-type SiNW

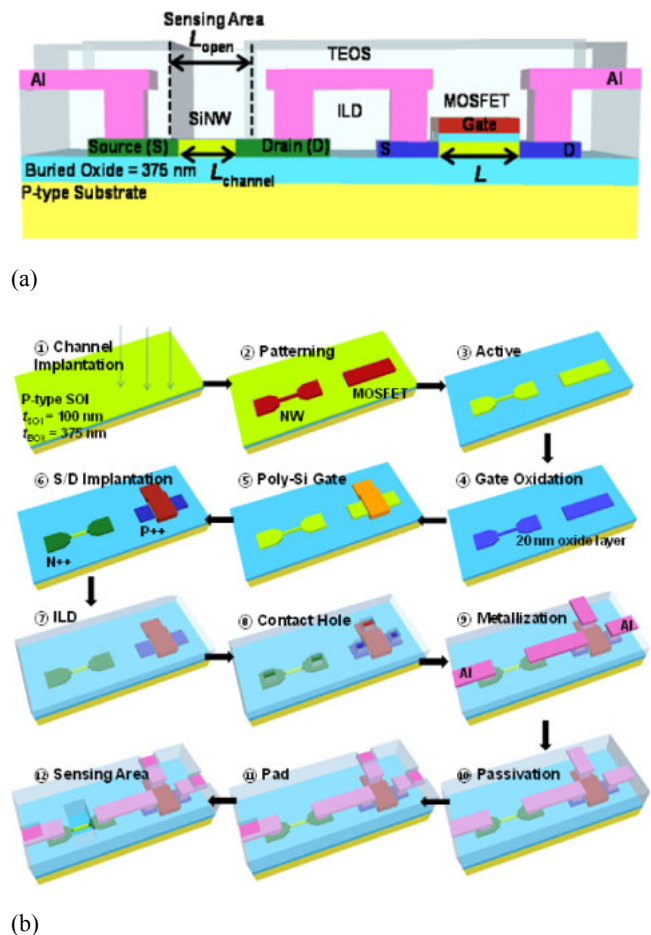


Fig. 1. (Color online) (a) Cross sectional schematic diagram and (b) fabrication process of the complementary SiNW ISFET with MOSFET.

ISFETs. Active region was patterned by mix-and-match (e-beam and photo) lithography to define nanowires and active pads (Fig. 2). After gate oxidation, the poly silicon gate was patterned only for the MOSFET because the channel region of SiNW biosensor must be exposed to electrolyte. Subsequently, source/drain implantation was conducted followed by a conventional back-end process including interlayer dielectric (ILD) deposition, contact/pad hole formation and metallization. Lastly, 300-nm-thick ILD oxide

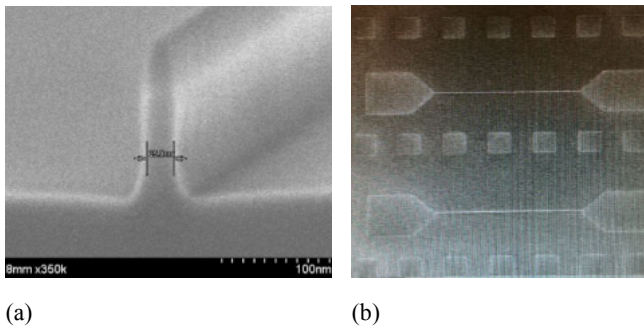


Fig. 2. (Color online) (a) Cross sectional and (b) top viewed scanning electron microscope images of nanowire patterned by mix-and-match lithography.

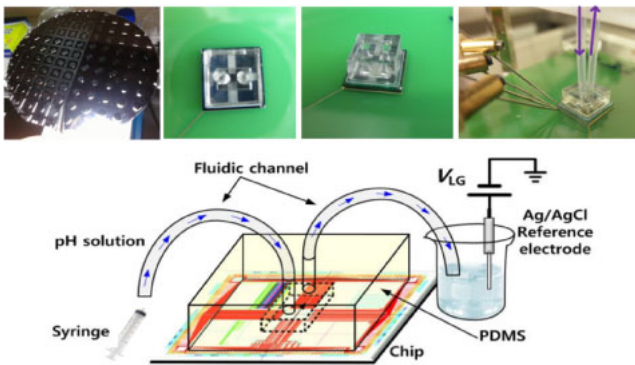


Fig. 3. (Color online) Measurement system for pH detection.

of SiNW biosensor region was removed by photolithography and RIE in CHF_3/CF_4 plasma to make a sensing area.

The measurement system of pH sensing is shown in Fig. 3. Poly(dimethylsiloxane) (PDMS) micro-fluidic channel was attached to the fabricated chip for the injection of pH solution. The surface of the channel was then treated with 3-aminopropyltriethoxysilane (3-APTES) to protect native oxide as well as to obtain linear sensitivity.⁵⁾

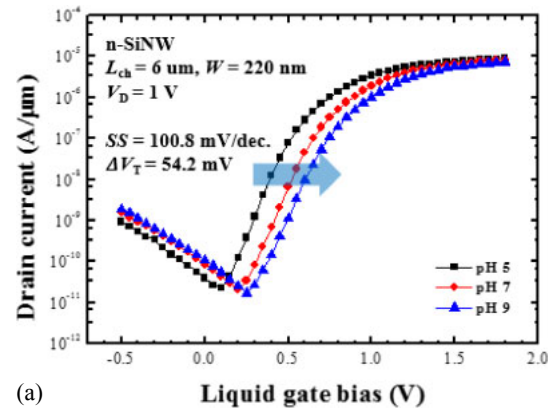
3. Results and discussion

3.1 Transfer characteristic as a pH sensor

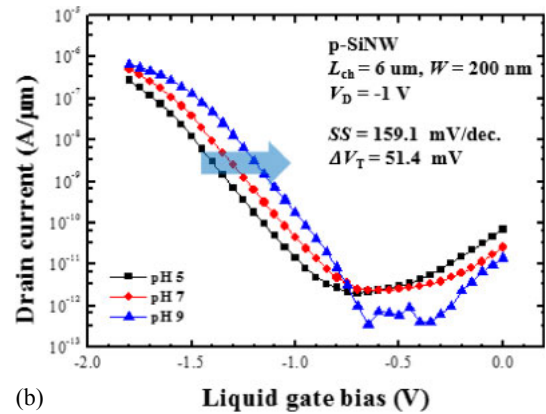
Transfer characteristics of fabricated n-channel SiNW (n-SiNW) and p-channel SiNW (p-SiNW) ISFETs with $L = 6\mu\text{m}$ and $W = 220\text{nm}$ were measured at various pHs. Potassium di-hydrogen phosphate (KH_2PO_4) and potassium mono-hydrogen phosphate (K_2HPO_4) were used as a buffer solution with hydrochloric acid (HCl) and potassium hydroxide (KOH). The drain biases of n-SiNW/p-SiNW were 1 and -1V , respectively. Figures 4(a) and 4(b) show the transfer characteristics measured in three different pH solutions. Average subthreshold swings (SS) are 100.8mV/decade for n-SiNW and 159.1mV/decade for p-SiNW. Threshold voltage shifts are 54.2 and 51.4mV/pH , respectively, which are close to the Nernst limit.²⁸⁾

3.2 Investigation of drift effect on n-SiNW pH sensor

Subsequently, transient measurements were conducted to investigate the drift effect of the ISFETs. The SiNW ISFETs were exposed to the pH solution with fixed liquid gate and drain biases. Figure 5(a) shows the result of n-SiNW measured for 500 s with $V_{LG} = 1.35\text{V}$ and $V_D = 1\text{V}$ at pH 9.

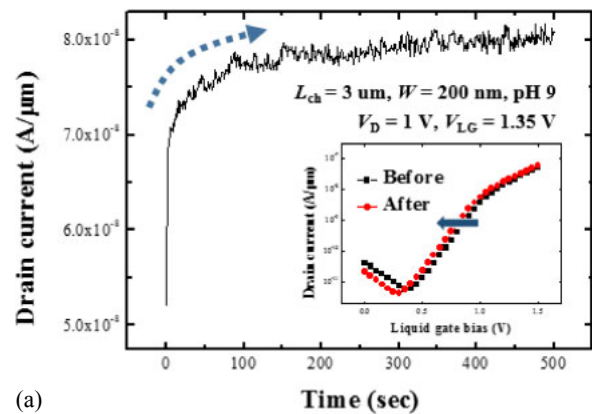


(a)

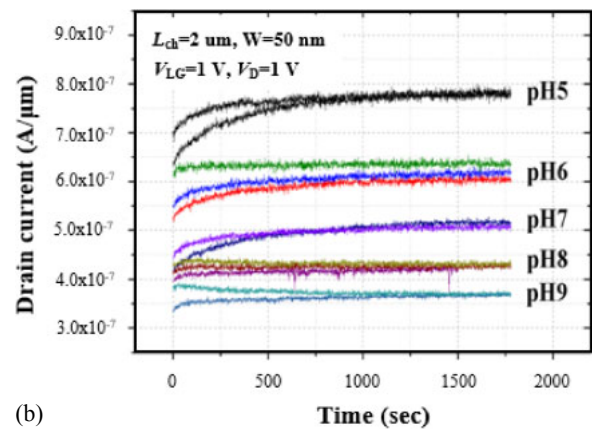


(b)

Fig. 4. (Color online) Transfer characteristics of (a) n-SiNW ISFET and (b) p-SiNW ISFET measured in various pH solutions.



(a)



(b)

Fig. 5. (Color online) (a) Transient characteristics and transfer curve changes (inset) of n-SiNW ISFET. (b) Transient characteristics of n-SiNW ISFET measured in five different pH solutions.

The drain current increases gradually for about 8 min without saturation, which indicates an unavailability of the reproducible detection. After 500s, the transfer characteristic was measured again as shown in the inset of Fig. 5(a). The threshold voltage was shifted to the negative direction. Moreover, as pH value decreases (concentration of hydrogen increases), the amount of the drift increases as depicted in Fig. 5(b). Considering the direction of the V_{th} shift, the polarity of the gate bias, and the drift dependency on pH, this slow response is evidently the result of positive species (H^+ ions) trapped at buried sites inside the insulator.^{20,26} H^+ ions diffuse into the insulator of ISFETs and combine with buried OH sites, resulting in a slowly changing channel potential. Contrast to surface sites binding, buried sites binding takes longer time to change their states due to relatively low diffusion constant of hydrogen ions in the oxide. It should be noted that the native oxide was used as a sensing insulator, which indicates vulnerability to ionic diffusion due to its porous attribute in comparison to other insulators such as pure oxide or high- k insulators.^{20,29}

3.3 Investigation of drift effect on p-SiNW pH sensor

However, in contrast to the n-SiNW, the p-SiNW shows completely different tendency. Figure 6(a) demonstrates that the drain current decreases gradually throughout the measurement. After the measurement, the threshold voltage was shifted to the negative direction and the subthreshold swing was increased fairly. Moreover, the amount of current drop increases with higher pH value (concentration of OH^- ions) and liquid gate bias as shown in Figs. 6(b) and 6(c). Based on these results, it is simply noticed that the current drift in the p-SiNW is related to the chemical reaction of OH^- ions with gate insulator. However, considering the direction of the V_{th} shift and the extremely small mobility of OH^- ion in the insulator,²⁵ the drift cannot be induced by the trapping of OH^- ions inside the insulator. The gate current was also measured to check if the insulator had been broken down by OH^- ions which are known to etch silicon dioxide. As seen in Figs. 7(a) and 7(b), the gate current was not changed throughout the transient measurement.

These phenomena can be explained by the chemical modification of insulator due to the surface reaction: hydration accelerated with OH^- ions.^{30,31} The reaction brings temporal decrease in the permanent dipole moment of the material, resulting in the decrease of oxide capacitance.²³⁻²⁵ Evidently, the degradation of subthreshold swing [inset of Fig. 5(b)] supports the hypothesis. The change of threshold voltage by the reduced insulator capacitance can be derived as follows:

$$\Delta V_T(t) = \Delta V_{FB}(t) + \Delta V_{OX}(t), \quad (1)$$

where ΔV_{FB} and ΔV_{OX} represent the flatband voltage and the voltage drop across the insulator. Conventional ΔV_{FB} and ΔV_{OX} equations can be substituted in Eq. (1) resulting

$$\Delta V_T(t) = -(Q_{OX} + Q_{ACC})[C_{OX}^{-1}(t) - C_{OX}^{-1}(0)], \quad (2)$$

where Q_{OX} is the density of charge inside the insulator and Q_{ACC} is density of accumulation charge stored in the channel. C_{OX} can be determined by the series combination of the hydrated layer capacitance and the underlying insulator capacitance. Detailed models are described in Refs. 24 and 25.

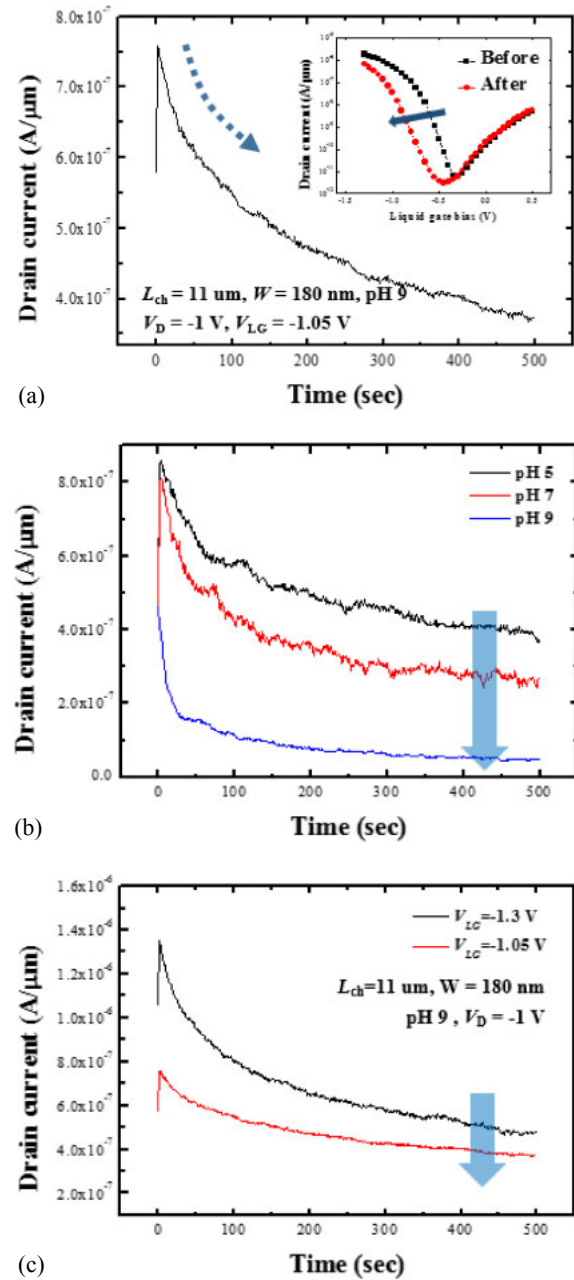


Fig. 6. (Color online) (a) Transient characteristics and transfer curve changes (inset) of p-SiNW ISFET. (b) Transient characteristics of p-SiNW ISFET measured in five different pH solutions. (c) Transient characteristics of p-SiNW ISFET measured at various gate biases.

Although the surface reaction may also occur in n-SiNWs, the current of n-SiNW continuously increases as a function of the measurement time since the current enhancement by H^+ diffusion completely compensates the current reduction by the surface reaction. This compensation can be proved by the fact that the amount of the V_{th} shift in n-SiNW is relatively smaller than that of p-SiNW as can be seen in the insets of Figs. 5(a) and 5(b).

4. Conclusions

The drain current drift was investigated in SiNW pH-sensitive ISFETs. Through the liquid gate bias and pH dependency of the ISFETs, the cause of the drift effect can be divided into two categories: 1) field-enhanced H^+ diffusion into the insulator and 2) chemical modification (hydration) of

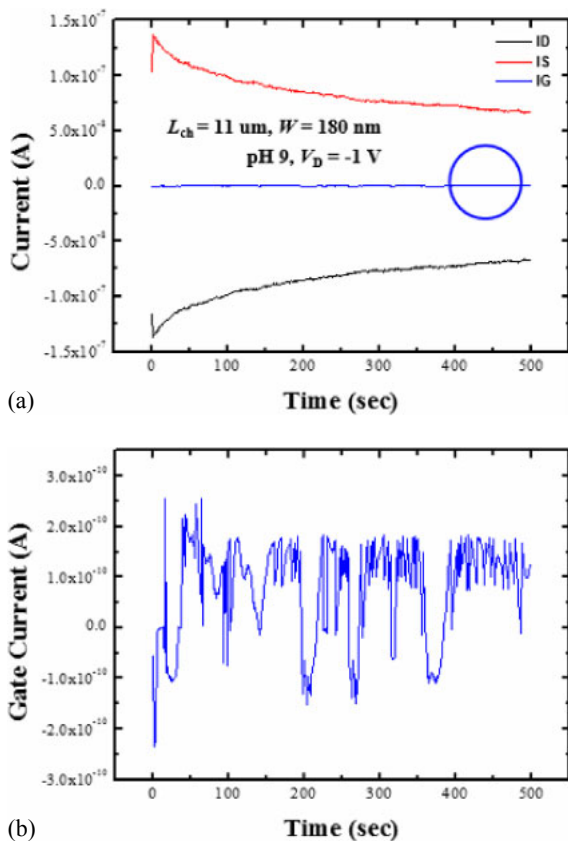


Fig. 7. (Color online) (a) Drain, source, and gate currents of p-SiNW ISFET measured during the transient measurement. (b) Enlarged gate current which is almost constant throughout the measurement.

the insulator. In n-SiNW, these mechanisms occur simultaneously but the current enhancement by the H^+ diffusion compensates the current reduction by the insulator modification. Thus, the drain current increases during the measurement time even though the hydration occurs. On the contrary, in p-SiNW, the drain current decreases throughout the measurement time because only the hydration occurs without OH^- diffusion into the insulator.

Acknowledgments

This work was supported by the Brain Korea 21 Plus Project in 2015 and National Research Foundation of Korea through the Ministry of Science, ICT and Future Planning (Grant No. 2013R1A1A2065339).

- 1) V. Mani, B. Devadas, and S. M. Chen, *Biosens. Bioelectron.* **41**, 309 (2013).
- 2) A. T. Sage, J. D. Besant, B. Lam, E. H. Sargent, and S. O. Kelley, *Acc. Chem. Res.* **47**, 2417 (2014).
- 3) C. Zhu, Z. Zeng, H. Li, F. Li, C. Fan, and H. Zhang, *J. Am. Chem. Soc.* **135**, 5998 (2013).
- 4) N. Chartuprayoon, M. Zhang, W. Bosze, Y. H. Choa, and N. V. Myung, *Biosens. Bioelectron.* **63**, 432 (2015).
- 5) Y. Cui, Q. Wei, H. Park, and C. M. Lieber, *Science* **293**, 1289 (2001).
- 6) M. A. M. Azmi, Z. Tehrani, R. P. Lewis, K.-A. D. Walker, D. R. Jones, D. R. Daniels, S. H. Doak, and O. J. Guy, *Biosens. Bioelectron.* **52**, 216 (2014).
- 7) A. Gao, P. Dai, N. Lu, T. Li, Y. Wang, S. Hemmila, and P. Kallio, *Int. Conf. Manipulation, Manufacturing and Measurement on the Nanoscale (3M-NANO)*, 2013, p. 333.
- 8) K. I. Chen, B. R. Li, and Y. T. Chen, *Nano Today* **6**, 131 (2011).
- 9) M. Y. Shen, B. R. Li, and Y. K. Li, *Biosens. Bioelectron.* **60**, 101 (2014).
- 10) L. Mu, Y. Chang, S. D. Sawtelle, M. Wipf, X. Duan, and M. A. Reed, *IEEE Access* **3**, 287 (2015).
- 11) G. Jayakumar, A. Asadollahi, P.-E. Hellström, K. Garidis, and M. Östling, *Int. Conf. Ultimate Integration on Silicon (ULIS)*, 2013, p. 81.
- 12) G. J. Zhang, H. H. Luo, M. J. Huang, G. K. I. Tay, and E. J. A. Lim, *Biosens. Bioelectron.* **25**, 2447 (2010).
- 13) A. Gao, N. Lu, Y. Wang, P. Dai, T. Li, X. Gao, Y. Wang, and C. Fan, *Nano Lett.* **12**, 5262 (2012).
- 14) T. Kong, R. Su, B. Zhang, Q. Zhang, and G. Cheng, *Biosens. Bioelectron.* **34**, 267 (2012).
- 15) G. Zheng, X. P. Gao, and C. M. Lieber, *Nano Lett.* **10**, 3179 (2010).
- 16) G. J. Zhang, M. J. Huang, J. A. J. Ang, Q. Yao, and Y. Ning, *Anal. Chem.* **85**, 4392 (2013).
- 17) X. T. Vu, R. GhoshMoulick, J. F. Eschermann, R. Stockmann, A. Offenhausser, and S. Ingebrandt, *Sens. Actuators B* **144**, 354 (2010).
- 18) J. H. Ahn, S. J. Choi, J. W. Han, T. J. Park, S. Y. Lee, and Y. K. Choi, *Nano Lett.* **10**, 2934 (2010).
- 19) L. H. Jiao and N. Barakat, *J. Nanosci. Nanotechnol.* **13**, 1194 (2013).
- 20) J. H. Lee, Dr. Thesis, Department of Electric and Computer Engineering, Seoul National University, Seoul (2014).
- 21) J. Lee, J. H. Lee, H. Jang, M. Uhm, W. H. Lee, S. Hwang, B. G. Park, I. Y. Chung, D. M. Kim, and D. H. Kim, *Proc. 19th Korean Conf. Semiconductors*, 2012, p. 435.
- 22) U. Hashim, S. W. Chong, and W.-W. Liu, *J. Nanomater.* **2013**, 542737 (2013).
- 23) S. Jamasb, S. D. Collins, and R. L. Smith, *Int. Conf. Solid State Sensors and Actuators*, 1997, p. 1379.
- 24) S. Jamasb, S. D. Collins, and R. L. Smith, *IEEE Trans. Electron Devices* **45**, 1239 (1998).
- 25) S. Jamasb, S. D. Collins, and R. L. Smith, *Sens. Actuators B* **49**, 146 (1998).
- 26) L. Bousse and P. Bergveld, *Sens. Actuators* **6**, 65 (1984).
- 27) J.-H. Ahn, J.-Y. Kim, C. Jung, D.-I. Moon, S.-J. Choi, C.-H. Kim, K.-B. Lee, H. G. Park, and Y.-K. Choi, *IEDM Tech. Dig.*, 2011, p. 852.
- 28) O. Knopfmacher, A. Tarasov, W. Fu, M. Wipf, B. Niesen, M. Calame, and C. Schonenberger, *Nano Lett.* **10**, 2268 (2010).
- 29) T. E. Bae, H. J. Jang, J. H. Yang, and W. J. Cho, *ACS Appl. Mater. Interfaces* **5**, 5214 (2013).
- 30) P.-Y. Chen, L.-T. Yin, M.-D. Shi, and Y.-C. Lee, *Life Sci. J.* **10**, 3132 (2013).
- 31) K. M. Chang, C. T. Chang, K. Y. Chao, and C. H. Lin, *Sensors* **10**, 4643 (2010).